

# A MUSE study of the inner bulge globular cluster Terzan 9: a fossil record in the Galaxy

H. Ernandes, B. Dias, B. Barbuy, S. Kamann, S. Ortolani, L. Rossi, E. Cantelli, E. Bica  
 Department of Astronomy, Universidade de São Paulo  
 {heitor.ernandes@usp.br}



## Overview

Globular clusters in the central parts of the Galaxy might be the oldest extant stellar population in the Milky Way (e.g. Barbuy et al. 2018; Kunder et al. 2018). Terzan 9 is a very compact cluster located at  $4^{\circ}12$  and 1.1kpc from the Galactic center, therefore in the inner bulge volume, and among the globular clusters closest to the Galactic center. see figure ?? . A metallicity of  $[Fe/H] \sim -2.0$  was deduced by Ortolani et al. (1999), and  $[Fe/H] \sim -1.2$  by Valenti et al. (2007) from Colour-Magnitude Diagrams. Vásquez et al. (2018) (ESO proposal 089.D-0493), measured the CaT lines and obtained  $[Fe/H] \sim -1.08$ ,  $-1.21$ , and  $-1.16$ , following calibrations from Dias et al. (2016), Saviane et al. (2012), and Vásquez et al. (2015) respectively. So the metallicity and properties for this cluster are in debate. These clusters are very old, around 13 Gyr, as deduced from proper-motion cleaned CMDs for example for NGC 6522 and HP 1 (Kerber et al. 2018a,b). This might indicate that the clusters formed early in the Galaxy, and were later trapped by the bar (see also Renzini et al. 2018)

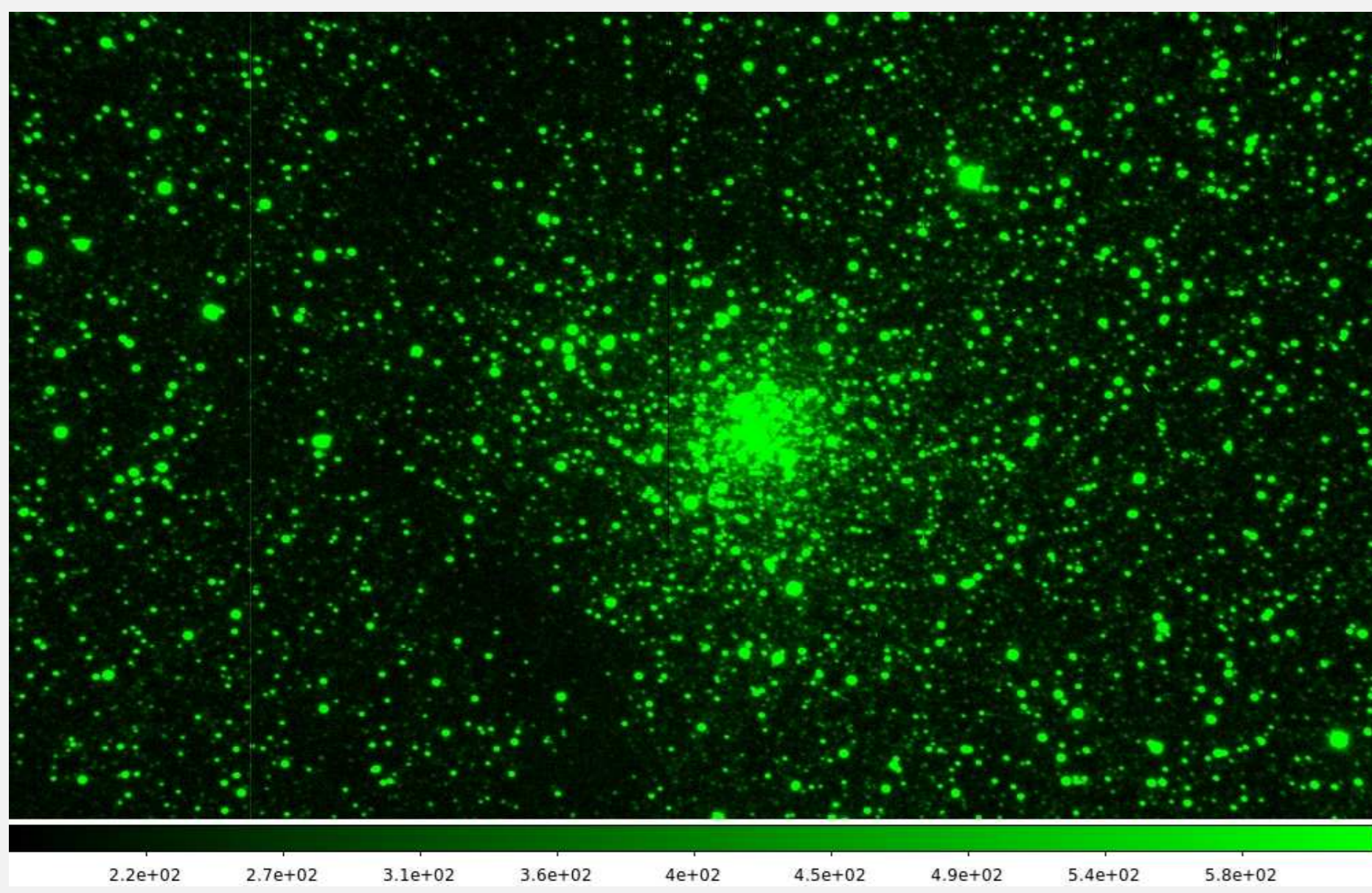


Figure 1: Image of Terzan 9 NTT.

## MUSE Data

Terzan 9 is a compact ( $r_{tidal} = 9.5'$  and concentration factor  $c = 2.50$ ) and faint. therefore a full imaging with the large MUSE IFU appears more suitable to identify member stars than multi-object spectrograph facilities. The observations of the Terzan 9 field were conducted with the MUSE instrument installed on UT4 "Yepun" of the Very Large Telescope, with the Wide Field Mode, no-AO, standard coverage (nominal mode WFM-NOAO-E). The FOV of MUSE in the Wide Field mode is  $1' \times 1'$  per exposure. The total observing time was 5 hours including overheads. see figure ??.

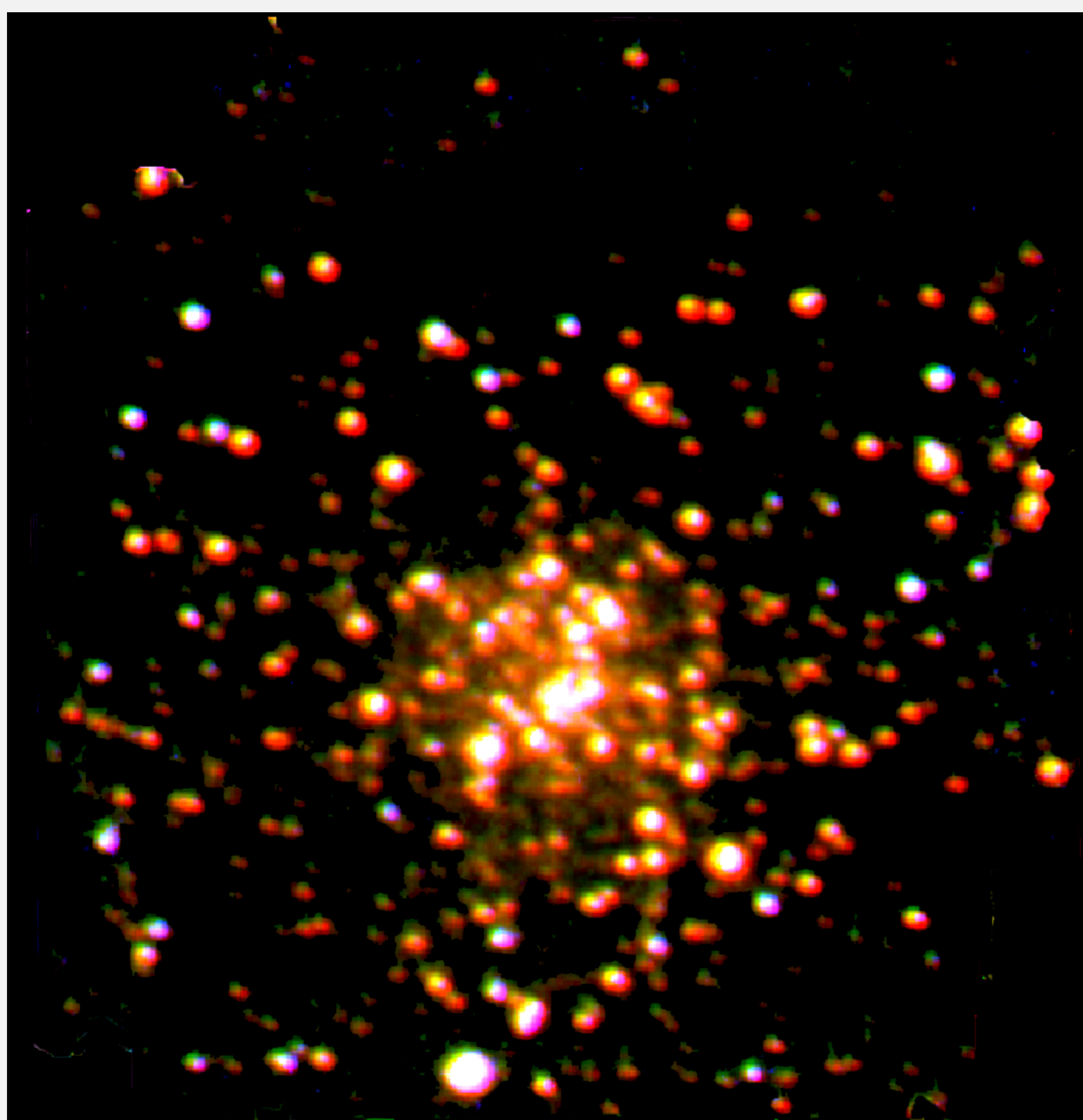


Figure 2: RGB image of Terzan 9 from a data cube of MUSE.

## Method

For extraction of stellar spectra the code PampelMUSE (Kamann et al. 2013), specific for spectra extraction in crowded fields of MUSE data cubes, was employed. This Software deals with the observation of a densely populated stellar field such as a globular cluster, which is our case. The challenge is the limited angular resolution of the instrument. A single object is represented by a point spread function (PSF). The code Etoile for extracting stellar parameters was built and presented by Katz et al. (2011). This code is a modified version of the code HALO (Cayrel et al. 1991): it compares to the full list of reference spectra and extracts the fundamental stellar parameters ( $T_{eff}$ ,  $\log g$ ,  $[Fe/H]$ ). See also Dias et al. (2015, 2016).

## Libraries

Dias et al. (2015, 2016) implemented two grids of spectra: the synthetic spectra by Coelho et al. (2005, hereafter Coelho05), and the MILES grid of observed spectra (Sánchez-Blázquez et al. 2006). In this paper we implemented Coelho05 with full wavelength coverage (3000-18000Å) so that we can use the full spectra from MUSE (4000-9000Å).

## Radial Velocity

Comparing diferents methods to derive radial velocity using the Etoile, we concluded the most reliable method to derive radial velocities is the comparison with the synthetic spectra in the CaII triplet (CaT) region 8400 - 8750 Å . The median radial velocity obtained is  $v_r = 45$  km/s and the mean heliocentric radial velocity is  $v_r = 53.4$ km/s. see figures ?? and ??.

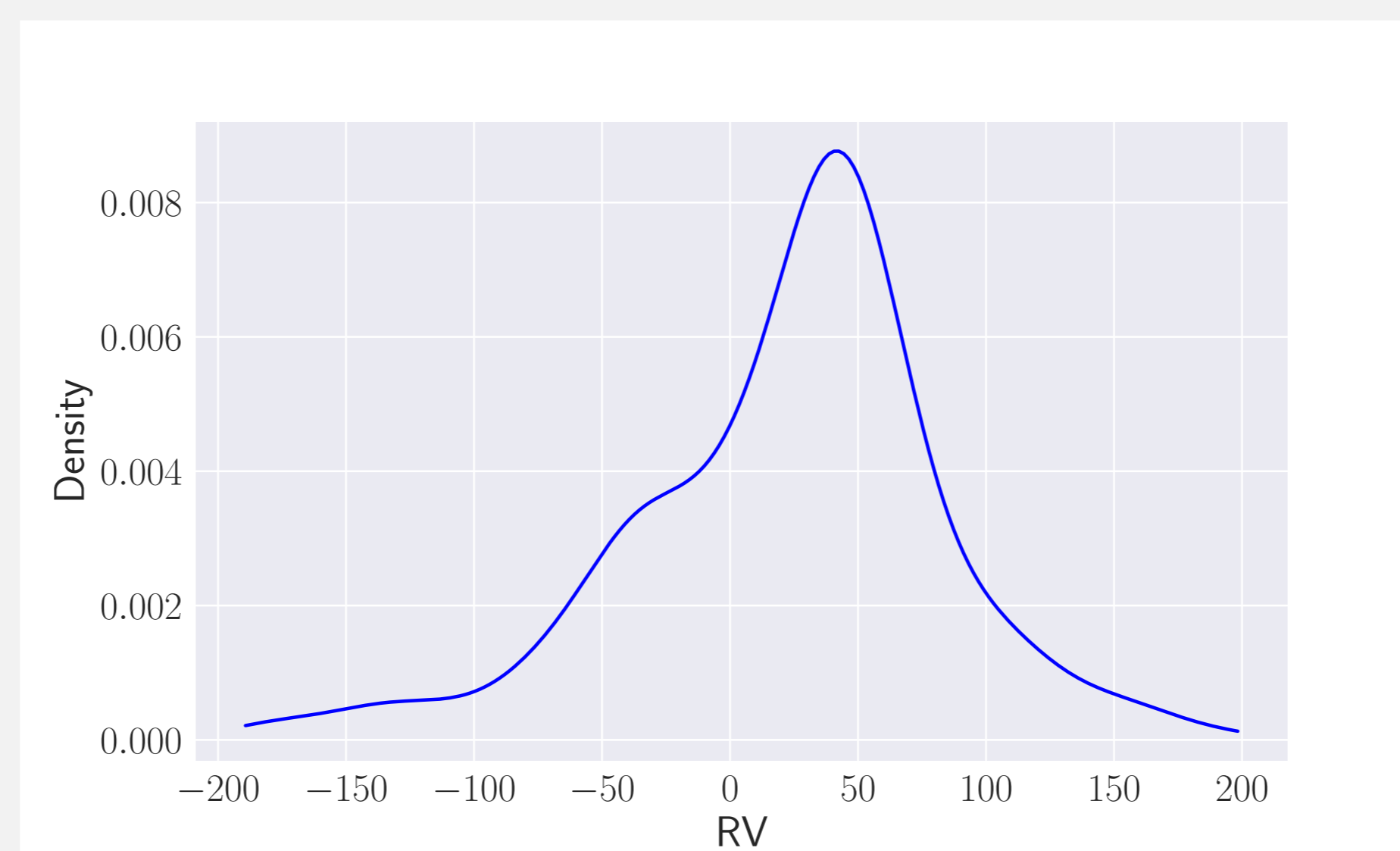


Figure 3: Radial Velocity distribution of Terzan 9.

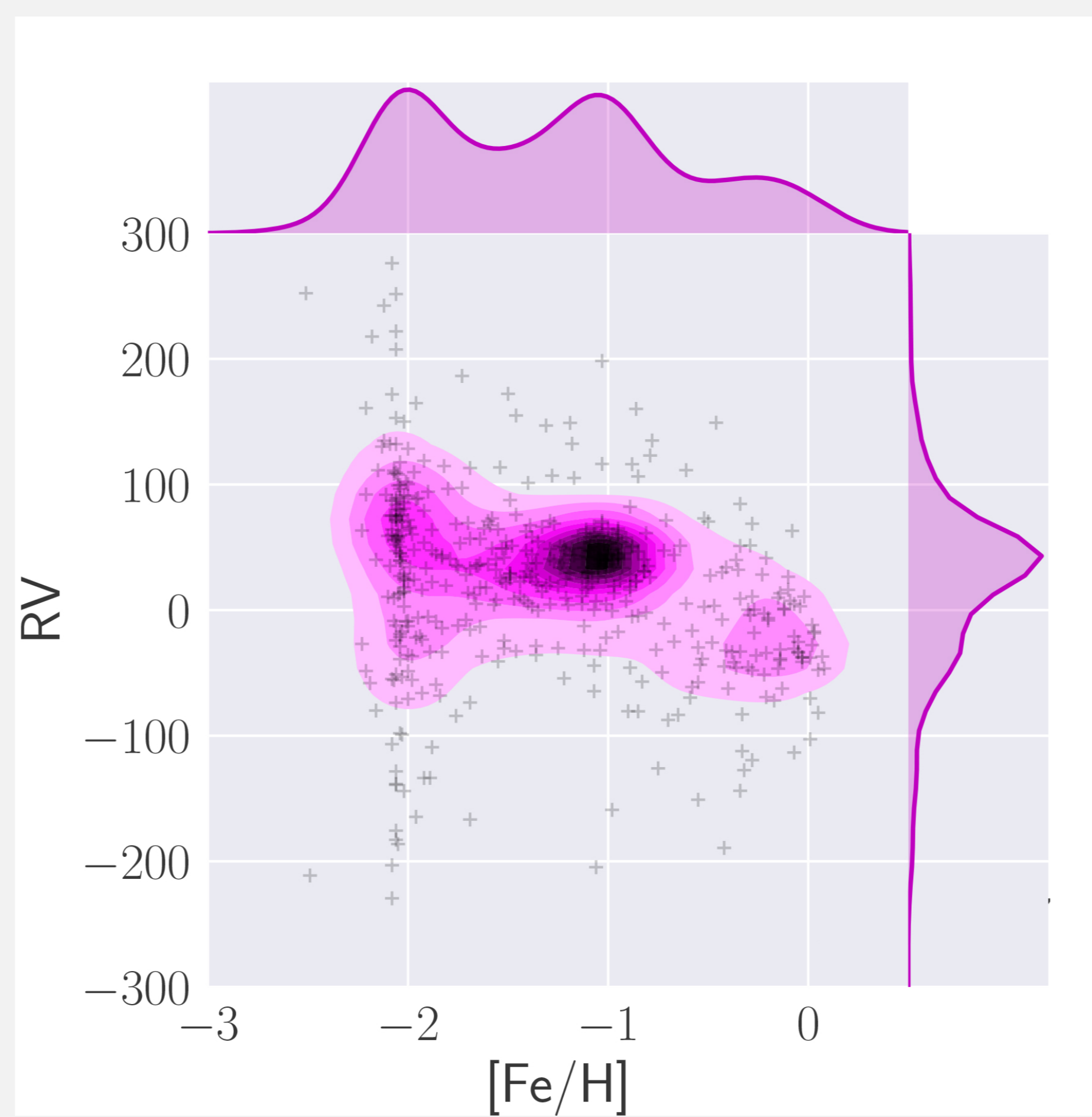


Figure 4: Radial Velocity distribution vs.  $[Fe/H]$  distribution for Terzan 9.

## Results

In the metallicity distribution we found  $[Fe/H] \approx -1.02$  for Terzan 9.

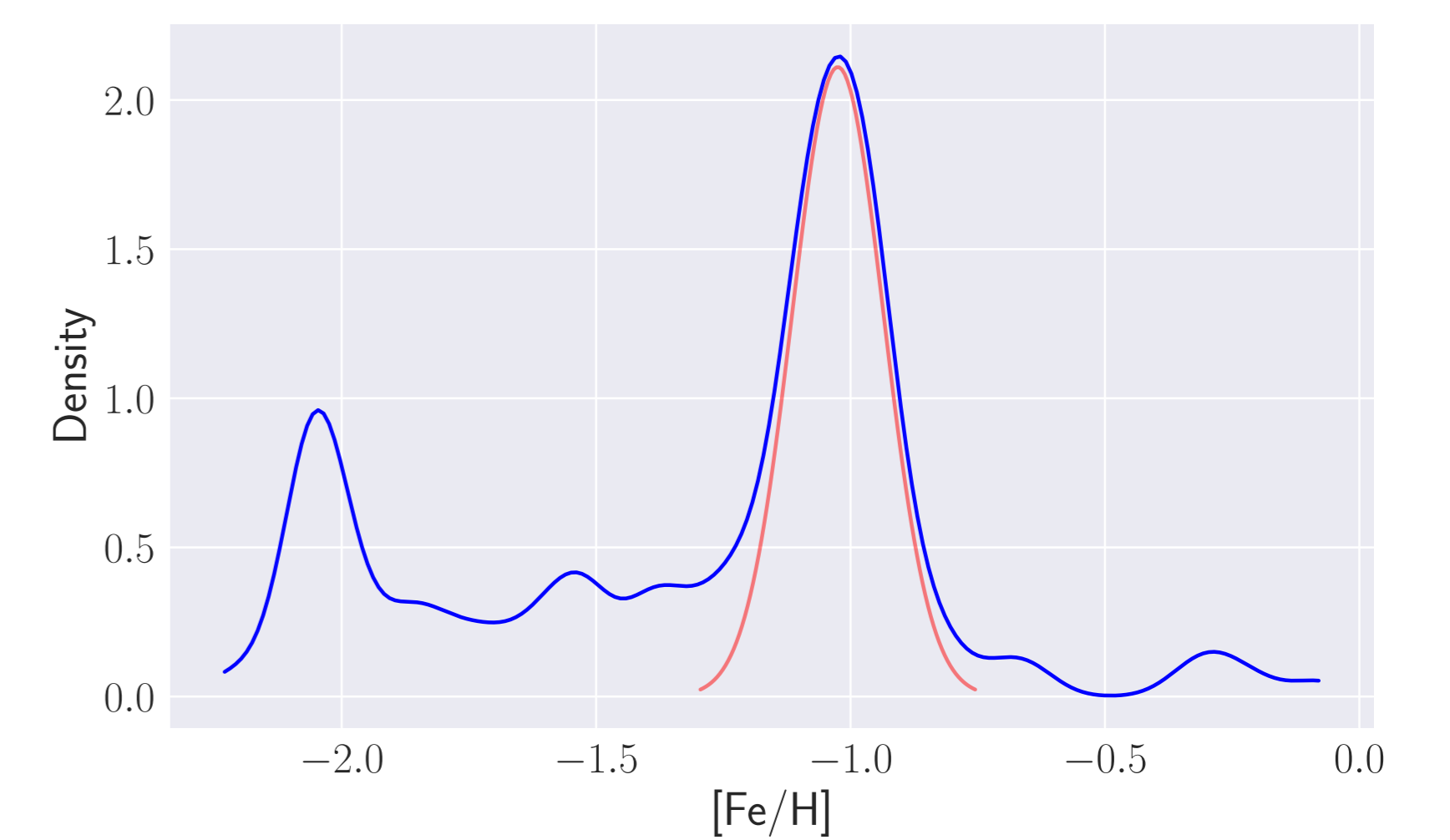


Figure 5: Metallicity distribution after RV selection.

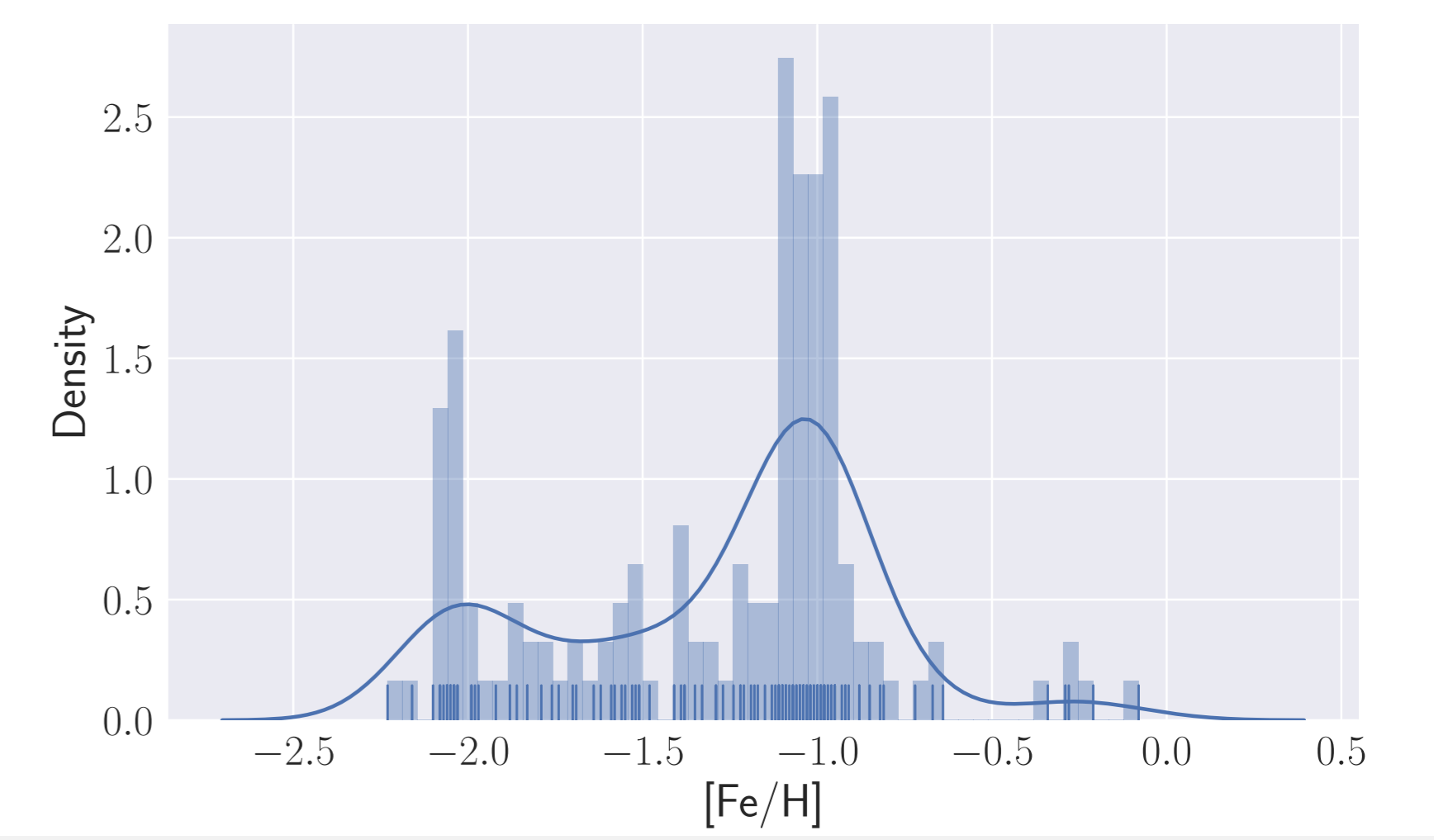
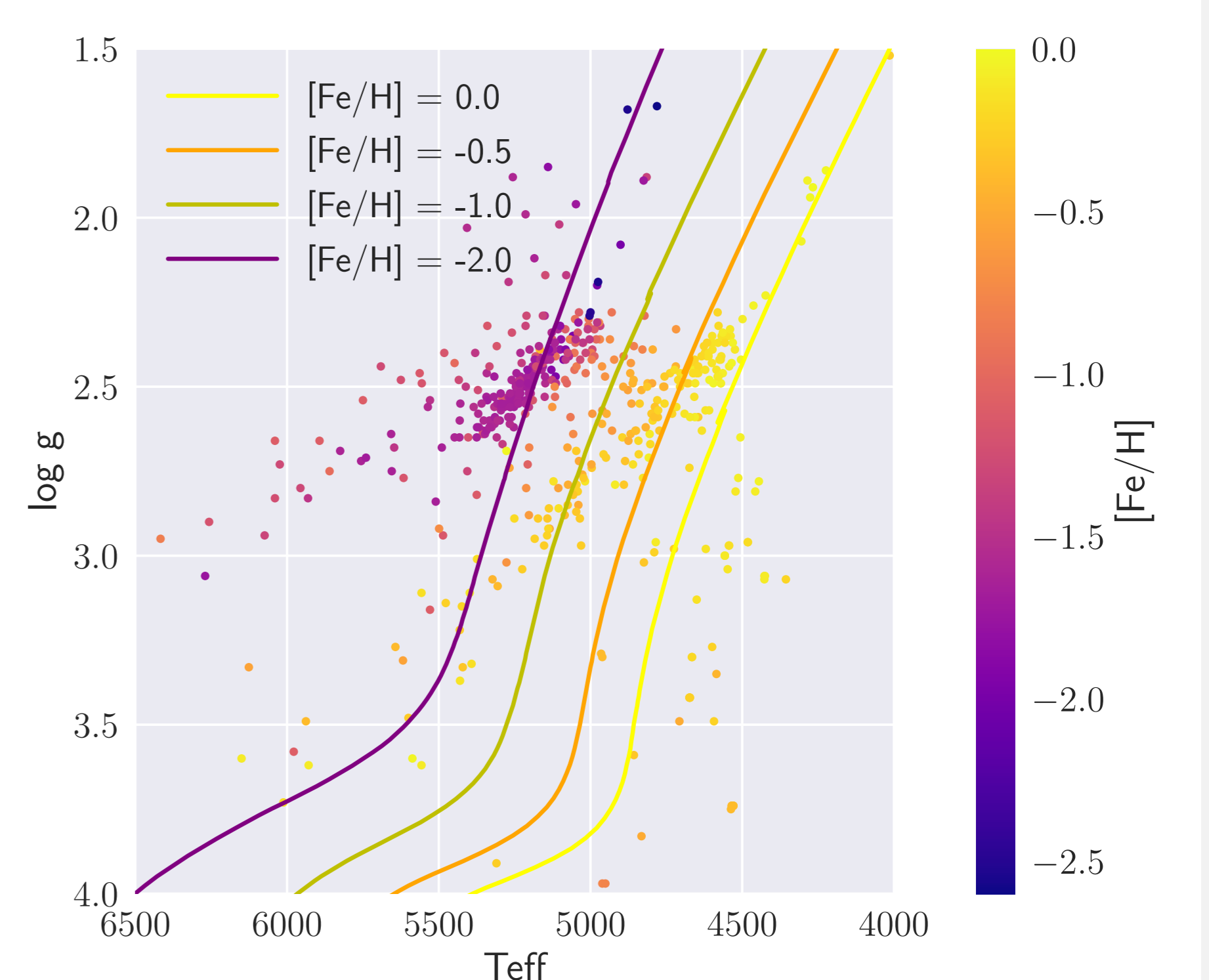
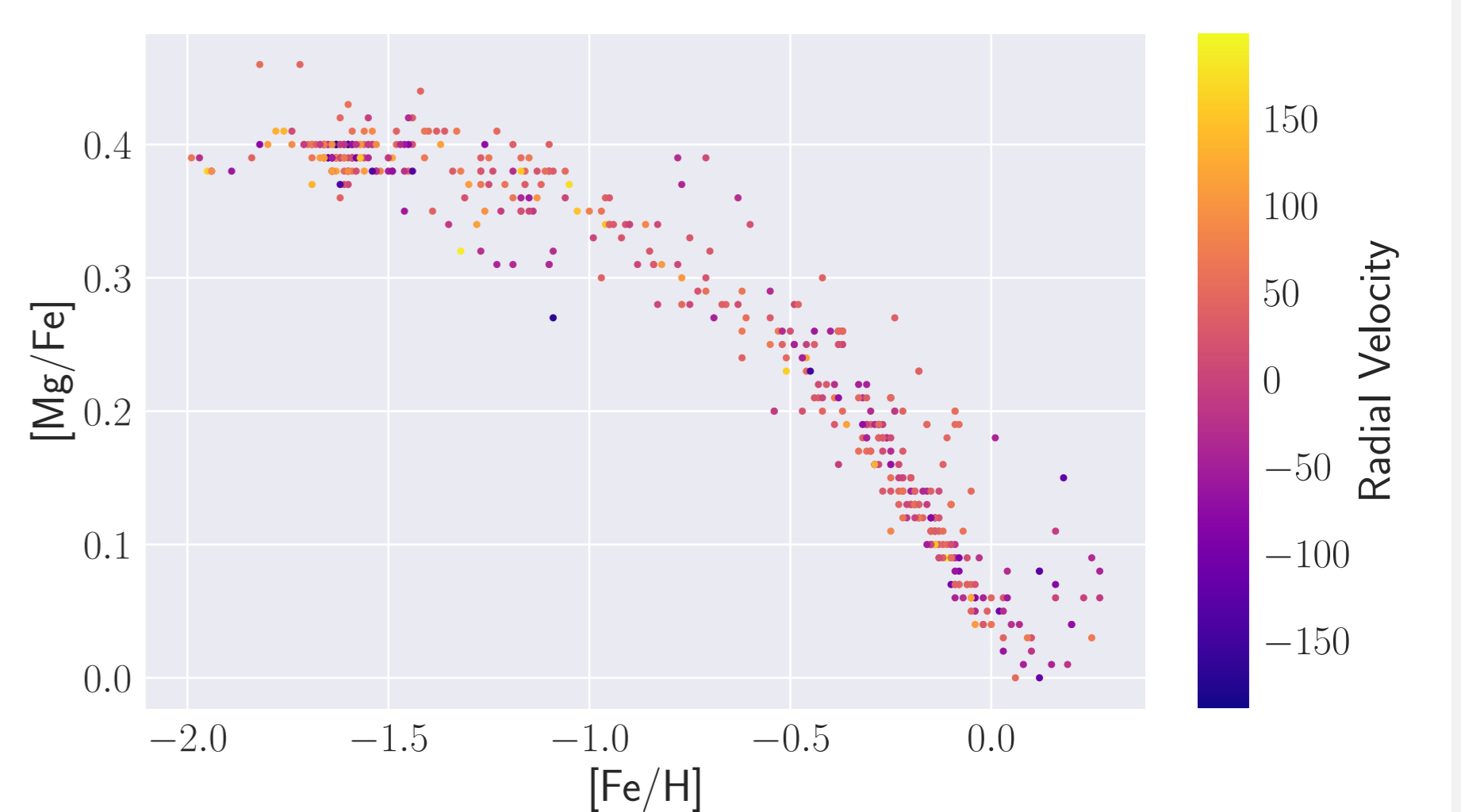


Figure 6: Metallicity distribution after RV selection.



## References

- Barbuy et al. 2018, A&A, 619, A178;
- Cayrel et al. 1991, A&A, 247, 108;
- Coelho et al. 2005, A&A, 443, 735; Dias et al. 2015, A&A, 573, A13;
- Dias et al. 2016, A&A, 590, A9;
- Kamann et al. 2013, A&A, 549, A71;
- Katz et al. 2011, A&A, 525, A90;
- Kerber et al. 2018a, ApJ, 853, 15;
- Kerber et al. 2018b, MNRAS, in press
- Kunder et al. 2018, SSRV, 214, 90;
- Ortolani et al. 1999, A&AS, 138, 267;
- Renzini et al. 2018, ApJ, 863 16;
- Sánchez-Blázquez et al. 2006, MNRAS, 371, 703
- Saviane et al. 2012, A&A, 540, A27;
- Vásquez et al. 2015, A&A, 580, A121
- Vásquez et al. 2018, A&A, 619, A13